Biochemical Pharmacology, Vol. 42, No. 11, pp. 2171–2180, 1991.
Printed in Great Britain.

0006-2952/91 $3.00 + 0.00
Pergamon Press plc

INVOLVEMENT OF GLUTATHIONE IN 1-NAPHTHYLISOTHIOCYANATE (ANIT) METABOLISM AND TOXICITY TO ISOLATED HEPATOCYTES

LAURIE CARPENTER-DEYO, DANIEL H. MARCHAND, PAUL A. JEAN, ROBERT A. ROTH* and DONALD J. REED†

Department of Biochemistry and Biophysics, Oregon State University, Corvallis, OR; and *Department of Pharmacology and Toxicology, Michigan State University, East Lansing, MI, U.S.A.

(*Received* 23 *March* 1991; *accepted* 19 *July* 1991)

Abstract—1-Naphthylisothiocyanate (ANIT) is a model compound which causes cholestasis in laboratory animals. Various biochemical and morphological changes including biliary epithelial and parenchymal cell necrosis occur in the liver of animals treated with ANIT. Although the mechanism(s) for these effects is not understood, a role for glutathione (GSH) in toxicity has been implicated. The possible role of GSH in hepatocellular toxicity caused by ANIT was investigated in this study. Treatment of freshly isolated rat hepatocytes with ANIT caused a concentration- and time-dependent depletion of cellular GSH that preceded lactate dehydrogenase (LDH) leakage. Analysis of the incubation medium indicated that the majority of the cellular GSH which was lost was present extracellularly as GSH or as a GSH-releasing compound. Mixing ANIT with GSH at pH 7.5 yielded a compound that was characterized by HPLC and fast atom bombardment–mass spectrometry (FAB–MS) as *S*-(*N*-naphthylthiocarbamoyl)-L-glutathione (GS-ANIT). When dissolved in aqueous solutions at neutral pH, 95% of GS-ANIT dissociated to yield free ANIT and GSH. Under conditions designed to maximize formation and stability of GS-ANIT, GS-ANIT was found in the extracellular medium of hepatocytes treated with ANIT. Treatment of hepatocytes with the GS-ANIT caused GSH depletion and LDH leakage similar to that observed with equimolar amounts of ANIT. These data suggest that ANIT depletes hepatocytes of GSH through a reversible conjugation process. Such a process may play a role in the toxicity of ANIT.

1-Naphthylisothiocyanate (ANIT‡) has been used for more than twenty years as a model compound to study mechanisms of intrahepatic cholestasis. When administered acutely to rats and mice, ANIT produces necrosis of bile ductular epithelial cells, followed by bile duct proliferation and bile stasis [1–4]. It has been suggested that these changes are consequences of the ability of ANIT to increase permeability of tight junctions of the biliosinusoidal barrier [5, 6].

In addition to affecting bile ductular cells, ANIT also induces morphologic and functional changes in hepatocytes. These changes include dilation of lamellae of Golgi, swelling and membrane damage in mitochondria, release of cytoplasmic enzymes, blebbing of plasma membranes, inhibition of bilirubin transport, and an impairment of microsomal mixed-function oxidase activity [7–11]. Because the hepatocyte is affected earlier than the bile ductular cells in the acute phase of ANIT intoxication, it has been suggested that the acute effects of ANIT in the liver are due to its effects on hepatocytes and not the bile ductular cells [4, 8].

Although the mechanism(s) of ANIT-induced cholestasis (or hepatocellular toxicity) is currently unknown, indirect evidence suggests that the cholestatic properties of ANIT may be due to a metabolite or metabolites. Microsomal enzyme inducers and inhibitors potentiate or ameliorate hyperbilirubinemia and cholestasis [12–14]. Bile duct ligation or cannulation also inhibits ANIT toxicity *in vivo* [15]. Furthermore, the disposition of ANIT in susceptible and nonsusceptible species differs [16]. Although urinary metabolites from susceptible species have been separated by thin-layer chromatography and characterized by R_f values [16], to date, none of the metabolic products of ANIT have been chemically identified and tested for toxicity.

In 1977, El-Hawari and Plaa [17] showed that pretreatment of rats with sulfhydryl compounds such as cysteine, cysteamine, and cystamine protects animals against ANIT-induced hyperbilirubinemia. These results suggest that ANIT may cause toxicity by depleting hepatocytes or bile ductular epithelial cells of reduced glutathione (GSH) or other thiols. In contrast, results of a recent study indicated that pretreatment of rats with GSH-depleting agents such as buthionine sulfoximine (BSO) and diethyl maleate (DEM) protects against ANIT toxicity [18]. These

† Corresponding author: Donald J. Reed, Ph.D., Department of Biochemistry and Biophysics, Oregon State University, 535 Weniger Hall, Corvallis, OR 97331-6503. Tel. 503-737-4438; FAX 503-737-0481.

‡ Abbreviations: ANIT, 1-naphthylisothiocyanate; GS-ANIT, *N*-naphthylthiocarbamoyl)-L-glutathione; GSH, reduced glutathione; GSSG, oxidized glutathione; PMR, proton magnetic resonance; PCA, perchloric acid; DBH, dibutylphthalate; LDH, lactate dehydrogenase; FAB–MS, fast atom bombardment–mass spectrometry; ACN, acetonitrile; MDA, malondialdehyde; BSO, buthionine sulfoximine; DEM, diethyl maleate; DMSO, dimethyl sulfoxide; and ANOVA, analysis of variance.

results suggest that the presence of GSH may promote, rather than inhibit ANIT toxicity.

In the past few years, it has become increasingly evident that GSH may be involved in bioactivation as well as detoxification of chemicals. GSH conjugates of both allyl and benzyl isothiocyanate have been found to produce toxicity in isolated rat liver epithelial cells [19, 20]. Based on results of these studies, we hypothesized that the toxicity of ANIT toward hepatocytes may be related to its conjugation with GSH. The results of experiments designed to test this hypothesis are described herein.

METHODS

Chemicals. All chemicals were purchased from the Sigma Chemical Co. (St. Louis, MO). Solvents were HPLC grade (OmniSolv, EM Science, Gibbstown, NJ) except for dimethyl sulfoxide (DMSO) (AR grade, Mallinckrodt Inc., Paris, KY) and deuterated NMR solvents which were purchased from the Aldrich Chemical Co. (Milwaukee, WI).

Synthesis of GS-ANIT. Thirty milligrams of ANIT (0.16 mmol) was dissolved in 1.0 mL of acetonitrile (ACN). Three hundred and fifty milligrams of GSH (1.10 mmol) was dissolved in 4.0 mL of 0.10 M Tris buffer (pH 7.0) and added dropwise to the ANIT solution over a 2-min period. After stirring at room temperature for 5 min, the pH of the reaction mixture was adjusted to <4 by the addition of 0.5 mL of glacial acetic acid. GS-ANIT was purified subsequently by injection of aliquots (0.5 mL) of the reaction mixture onto a 9.6 × 300 mm reverse-phase C18 HPLC column (Custom LC, Houston, TX) followed by elution with a 20% ACN–0.1% acetic acid mobile phase delivered at 3.0 mL/min. The post-column effluent was monitored at 308 nm for the presence of GS-ANIT. Under these conditions, GS-ANIT began eluting at 17 min, at which time the post-detector effluent was frozen by diverting it to a lyophilization flask immersed in liquid nitrogen. Repeated collections of GS-ANIT in this fashion were followed by lyophilization of the frozen material, and the resulting solid was stored at −80° until needed.

Verification of the synthesized material was achieved by fast atom bombardment–mass spectrometry (FAB–MS) and thin-layer chromatography (TLC). FAB–MS (negative mode) analysis which was carried out on a Kratos MS50TC RF mass spectrometer was with samples dissolved in either water, ACN, or a combination of water, ACN, and acetic acid, placed in a glycerol matrix, and desorbed with a 7 kV xenon neutral beam. For TLC analysis, samples were spotted on silica gel G TLC plates (Analtech, Newark, DE) and developed with isopropyl alcohol/water/acetic acid (85/14/1). Plates were visualized under UV light and ninhydrin spray (0.15% in acetone). R_f values were 0.31, 0.26, and 0.91 for GS-ANIT, GSH, and ANIT, respectively. Analysis by proton magnetic resonance (PMR) of samples of GS-ANIT dissolved in either D_2O/0.01% D_4-acetic acid or D_2O/35% D_3-ACN/0.1% D_4-acetic acid were unsuccessful in that the peak splitting resulting from spin–spin couplings was generally unresolved. However, two sets of signals were visible: one, in the aromatic region of the PMR spectrum; the other, in the region which would be considered characteristic of peptides such as GSH.

Stability of ANIT and GS-ANIT. The stability of ANIT and GS-ANIT was determined by UV and HPLC analysis. UV spectra of ANIT (0.67 mM) and GS-ANIT (0.67 mM) in 20% ACN–0.05 M sodium phosphate (pH 7.5) or 20% ACN–0.1% acetic acid (pH < 3.5) were obtained with a DW-2000 dual-beam UV-Vis spectrophotometer (SLM-Aminco, Urbana, IL). For HPLC analysis, ANIT (0.11 mM) and GS-ANIT (0.15 mM) were dissolved in 35% ACN–0.05 M potassium phosphate buffer (pH 7.5) or 35% ACN–0.1% acetic acid (pH < 3.5). All incubations were carried out in capped 1.5-mL polypropylene microcentrifuge tubes at 25°. At various times following the initial addition of ANIT or GS-ANIT to the incubation mixture, the tubes were vortexed and 0.03-mL aliquots were removed and diluted in 0.57 mL of 35% ACN–0.1% acetic acid. Preliminary studies showed that less than 3% of ANIT or GS-ANIT was lost over a 10-hr period under these conditions. In some experiments, a 5-fold excess of GSH was added to the incubation mixture prior to the addition of ANIT or GS-ANIT.

The concentration of ANIT and GS-ANIT was determined by introducing either 0.020 mL or 0.125 mL of the samples onto a 4.6 mm × 25 cm, reverse-phase C18 HPLC column (5 μm ODS, Custom LC). A mobile phase consisting of 35% ACN–0.1% acetic acid was delivered at 1.0 mL/min. Separation and elution of the various components were achieved by linearly increasing the ACN content of the mobile phase to 80% over a 10-min interval following sample injection. Under these conditions, GS-ANIT eluted at 9.0 min ($K' = 5$) and ANIT at 17 min ($K' = 11$). To ensure that a fixed amount of sample was being examined, a filled-loop method of repetitive injections was used. The presence of ANIT and GS-ANIT in the post-column effluent was detected at 308 nm.

Instrumentation for HPLC analyses. The HPLC solvent delivery system was either an Altex 100A dual-pump HPLC (Berkeley, CA) controlled by an Altex 420 solvent programmer or a Spectra Physics SP8700 HPLC (San Jose, CA). Sample injection was performed manually with a fixed loop, six-port injector (Valco Instruments Inc., Houston, TX), or automatically with a Micromeritics 728 autosampler (Norcross, GA). The presence of UV-absorbing material in the post-column effluent was monitored with a variable wavelength Kratos Spectroflow 757 UV detector or a 4120 Rapid Spectral UV detector (LKV, Bromma, Sweden) which was set to scan from 250 to 350 nm in 2-nm steps at 0.5-sec intervals (integration time of 0.5 sec). The peak areas were integrated with either a Hewlett–Packard 3390A (Avondale, PA) or a Shimadzu CR5A Chromatpac (Kyoto, Japan) Integrator.

Preparation and treatment of hepatocytes. Parenchymal cells were isolated from the livers of anesthetized, male, Sprague–Dawley rats (180–200 g) by collagenase perfusion [21]. They were resuspended in modified Fisher's medium (minus sulfur-containing amino acids) containing 2.5 mM Ca^{2+} at a concentration of 2×10^6 cells/mL. Initial

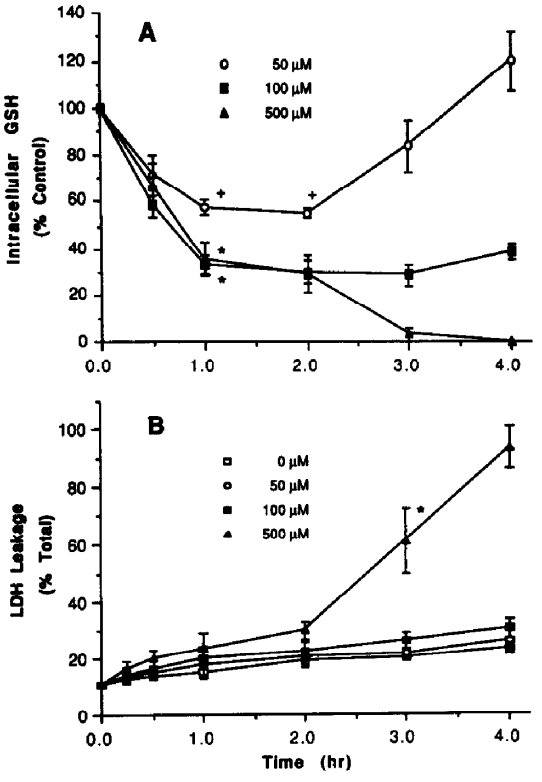

Fig. 1. Effect of ANIT on (A) intracellular GSH content and (B) LDH release from isolated hepatocytes. Hepatocytes in suspension were treated with ANIT (50, 100 or 500 μM) or DMSO vehicle and were analyzed for GSH and LDH release as described in Methods. Intracellular GSH is corrected for cell number and is expressed as percent of control at each time point. The initial and final GSH levels in the control cells were 13.5 ± 3.4 and 7.8 ± 1.5 nmol/10^6 cells, respectively. LDH release is expressed as percent total LDH released by 0.04% Triton X-100. (The average value for this parameter was 1.995 units/mL). Data are means ± SEM; N = 3–4 for each group. Key: (*) significantly different from control at this and subsequent time points ($P < 0.05$); (+) significantly different from control at only these time points ($P < 0.05$).

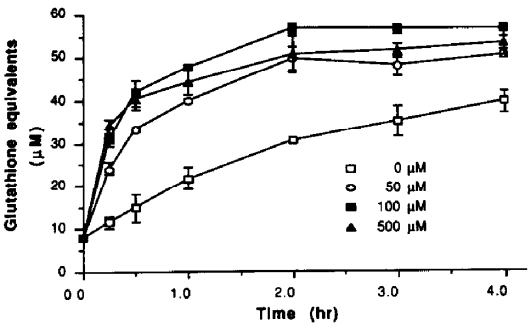

Fig. 2. ANIT-induced accumulation of extracellular glutathione from hepatocytes. Cells in suspension were treated with ANIT (50, 100 or 500 μM) or DMSO vehicle and the medium was analyzed for GSH and GSSG as described in Methods. Values are expressed as nmol glutathione equivalents (GSH + 2 GSSG) per mL of medium (μM). Data are means ± SEM, N = 3 for each group. Data points from hepatocytes treated with ANIT (all concentrations) were significantly different from control at all time points (except time 0) ($P < 0.05$).

viability, as assessed by trypan blue exclusion, was >90% for all experiments.

Aliquots of cell suspension (15 mL) were treated with vehicle (DMSO, 100 μL), ANIT, or GS-ANIT at various concentrations. Cells were then placed in an incubator (37°) and were rotated slowly under an atmosphere of 95% O_2/5% CO_2 for up to 4 hr. Aliquots of cell suspension were taken from each flask prior to and at various times during the incubation period for analysis of lactate dehydrogenase (LDH) release, malondialdehyde (MDA) formation, intracellular and extracellular reduced and oxidized glutathione (GSH and GSSG, respectively), and GS-ANIT conjugate formation (as described below).

To determine whether a GS-ANIT conjugate was formed during incubations of hepatocytes with ANIT, cells (5×10^6/mL) were treated with 1.0 mM ANIT, and at various times 1.5 mL of the cell suspension was centrifuged at 12,000 rpm to pellet the cells. An aliquot (0.5 mL) of the supernatant was removed and immediately frozen in liquid nitrogen. Following lyophilization, the samples were dissolved in 0.20 mL of 35% ACN containing either 1.0 M sodium acetate (pH 4.0) or 0.05 M sodium phosphate (pH 8.0) and centrifuged to remove any insoluble material prior to HPLC analysis as described above. A mobile phase of 0.05 M sodium acetate (pH 4.0)–10% ACN was substituted to reflect the differences in sample preparation. After injection of samples, the ACN content of the mobile phase was linearly increased to 70% over a 15-min interval. Under these conditions, GS-ANIT eluted at 11 min ($K' = 9$) and ANIT at 30 min ($K' = 29$).

Biochemical analyses of hepatocytes. Separation of live cells from dead cells and medium was achieved by centrifuging an aliquot of cell suspension through a layer of dibutyl phthalate (DBH) and into 10% perchloric acid (PCA) as previously described [21]. The content of GSH and GSSG in the medium above the DBH (extracellular) and in the PCA extract (intracellular) was determined by the HPLC method of Reed *et al.* [22]. Briefly, this method involves the addition of 2-iodoacetic acid followed by the derivatization of the *S*-carboxymethyl products with 2,4-dinitrofluorobenzene. Concentrations of derivatized GSH and GSSG were determined by UV detection (365 nm) following separations on a propylamine HPLC column. Intracellular GSH and GSSG values were corrected for the number of viable cells which came through the DBH as determined by the DNA content of the PCA precipitate [23] and are expressed per 10^6 cells. Lactate dehydrogenase (LDH) activity in the medium above the DBH was measured as previously described [24]. It is expressed as maximal LDH release elicited by treatment of cells with Triton X-100 (0.04%). Lipid peroxidation was assessed by assaying an aliquot (0.25 mL) of cell suspension for MDA [25].

Statistics. Data were analyzed using a one-way analysis of variance (ANOVA) program from Statview (Brainpower, Inc., Calabasas, CA), and means were compared by a Dunnett's *t*-test. $P < 0.05$ was chosen as the level of significance. Data are presented as means ± SEM.

RESULTS

Toxicity of ANIT towards hepatocytes in vitro. When exposed to ANIT, isolated hepatocytes underwent a time- and concentration-dependent depletion of intracellular GSH as seen in Fig. 1A. This depletion occurred as early as 30 min after incubation of cells with 100 μM ANIT. Whereas the GSH concentration recovered to control levels in cells treated with 50 μM ANIT after 4 hr of incubation, GSH levels were 35 and 0% of control in cells treated with 100 or 500 μM ANIT, respectively. As shown in Fig. 1B, treatment of cells with 500 μM, but not 100 μM ANIT produced an appreciable loss of cell viability as measured by the release of LDH. This loss of cell viability was not associated with an increase in lipid peroxidation as assayed by MDA formation (data not shown).

As depicted in Fig. 2, treatment with ANIT was associated with an accumulation of glutathione in the extracellular medium. In both control and ANIT-treated cells, more GSH equivalents were present in the medium at 4 and 2 hr of incubation, respectively, than were originally present in the cells. This is likely due to release of GSH synthesized within the cells during the experiment [26]. In contrast to intracellular GSH depletion, GSH accumulation in the incubation medium did not appear to occur in a concentration-dependent manner. All concentrations caused a similar increase in total glutathione content of the medium at all time points assayed. Although not shown in the figure, at early times, most of the glutathione present in the medium of cells treated with ANIT was reduced (GSH). Furthemore, whereas the concentration of GSH in the medium of cells treated with ANIT was greater than that of the control at all times prior to 4 hr, the concentration of GSSG was not different from control until 4 hr.

Synthesis of GS-ANIT. To determine if ANIT reacted directly with GSH, the disappearance of ANIT in the absence or presence of GSH was monitored by reverse-phase HPLC. In the absence of GSH, approximately 10% of ANIT disappeared from a 35% ACN–0.05 M phosphate buffer (pH 7.5) over a 1-hr period. The addition of a 5-fold excess of GSH (relative to ANIT) to the buffer resulted in an initial increase in the rate of disappearance of ANIT. The disappearance of ANIT in the presence of GSH coincided with the appearance of an unidentified peak which eluted prior to ANIT. This peak was not apparent in samples of ANIT only. The fact that this peak eluted prior to that of ANIT indicated that it was a polar product, possibly resulting from the conjugation of GSH with ANIT. This conclusion was confirmed in the following manner.

The peak tentatively assigned to GS-ANIT was collected from a preparative HPLC column and immediately frozen by diverting the post-column effluent into a container immersed in liquid nitrogen. Following lyophilization, the dehydrated material was analyzed by FAB–MS. Analysis by FAB–MS (negative ion mode) produced a spectrum (Fig. 3) in which the predominant signals were at m/z 306 (the base peak) and at m/z 491. This latter signal, the intensity of which was 20% of the base peak, was assigned to the parent ion (M-1) of GS-ANIT. A number of weaker signals were also observed originating as either pseudo-ions from the addition of the glycerol matrix or sodium to GS-ANIT, or the fragmentation of GS-ANIT. Particularly significant were the signals at m/z 274 and 218 which most likely arose from cleavage of the thiol and β-carbon bond of the cysteinyl portion of GS-ANIT. This suggests that ANIT is covalently attached to the thiol of GSH rather than to the amine of GSH. This conclusion was also supported by TLC analysis of product, which indicated that it was sensitive to detection by both UV and ninhydrin. Neither ANIT nor GSH was apparent in samples of product which were examined by TLC.

The base peak at m/z 306 observed in the FAB–MS spectrum of GS-ANIT (Fig. 3) may have arisen from either the presence of GSH (mol. wt 307) resulting from dissociation of GS-ANIT to GSH and ANIT, or possibly a daughter ion fragment of the parent compound. The weak signal at m/z 186 (i.e. ANIT) would appear to indicate that only a small amount of ANIT was present in the mixture; however, subsequent work examining ANIT itself by FAB–MS revealed that ANIT alone produced little or no parent ion signal. FAB–MS analysis of an equimolar mixture of GSH and ANIT produced a spectrum in which the base peak was also at m/z 306. A signal at m/z 491 was observed but was less than 5% of the intensity of the base peak.

Reversion of GS-ANIT to GSH and ANIT. Samples of GS-ANIT that were dissolved in 20% ACN–0.05 M phosphate buffer (pH 7.5) and immediately examined by UV spectroscopy showed a maximum absorbance at 282 nm (Fig. 4, top); a subsequent analysis of the same sample 15 min later indicated that a shift in the maximum absorbance to 308 nm had occurred. The resulting spectrum was similar to that produced by ANIT (Fig. 4, bottom). In contrast, samples of GS-ANIT that were dissolved in 20% ACN–0.1% acetic acid (pH < 3.5) showed little change over a 15-min period (results not shown).

Examination of GS-ANIT by HPLC gave similar results. A rapid disappearance of GS-ANIT was observed when the conjugate was dissolved in 35% ACN–0.05 M phosphate buffer, pH 7.5 (Fig. 5). The disappearance of GS-ANIT resulted in the concomitant appearance of ANIT. Within 5 min, an apparent equilibrium between ANIT and GS-ANIT was reached, with 95% of the ANIT present in the free form. Under these conditions, the amount of GS-ANIT then remained constant up to the end of the 1-hr incubation period. The equilibrium constant for GS-ANIT ↔ GSH + ANIT was calculated to be 2.7. As would be expected, the presence of 5-fold excess GSH shifted the process in favor of GS-ANIT whereupon 20% of the initial GS-ANIT was still

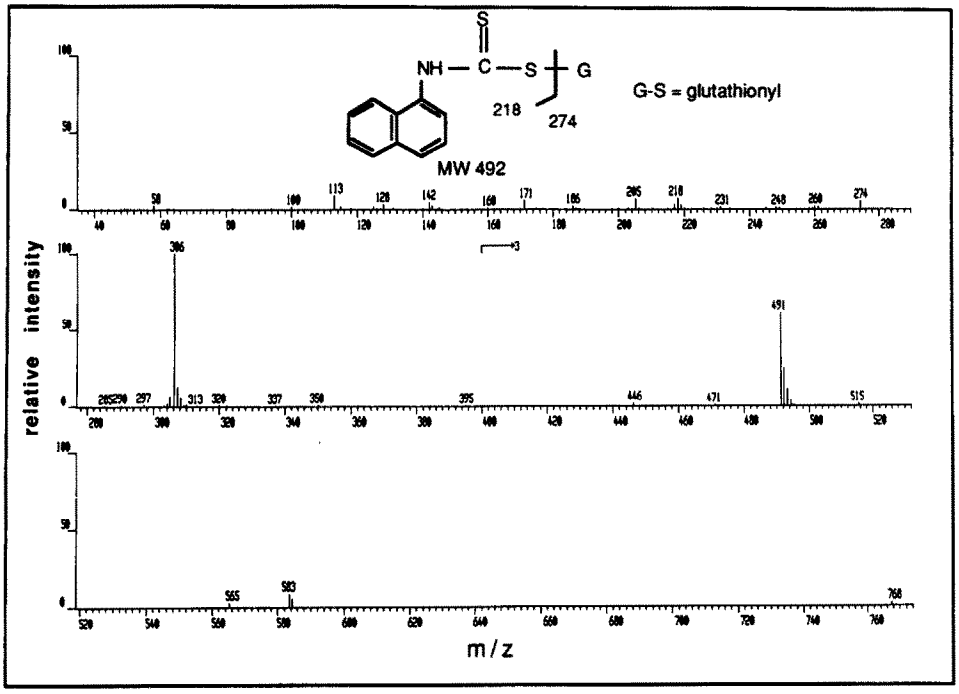

Fig. 3. FAB–MS spectrum (negative ion mode) of GS-ANIT placed in a glycerol matrix. The background signals originating from the glycerol matrix were subtracted. Note that the intensity of signals $>m/z$ 400 are magnified 3-fold. The peak at m/z 491 corresponds to that predicted for the molecular ion of GS-ANIT (structure as shown).

present as the conjugate at equilibrium. When GS-ANIT was dissolved in 35% ACN–0.1% acetic acid (pH < 3.5), less than 3% disappeared over a 10-hr period (results not shown). These results indicate that the GS-ANIT conjugate is reversible in nature, resulting in the formation of ANIT, and that this dissociation is dependent on pH.

Identification of GS-ANIT in vitro. The extracellular medium of hepatocytes treated with ANIT was examined for the presence of GS-ANIT. At various times following the addition of ANIT, aliquots of the cell incubations were centrifuged to remove the cells, and the supernatant was frozen immediately with liquid nitrogen. Following lyophilization, HPLC analysis of samples revealed the presence of a peak with a retention time of 11.0 min which was identical to that of GS-ANIT (Fig. 6A). If the dehydrated material was dissolved in 35% ACN–1.0 M sodium acetate (pH 4.0) prior to HPLC analysis, the size of this peak remained constant. However, dissolving the dehydrated material in 35% ACN–0.05 M sodium phosphate (pH 7.5) 1 hr prior to HPLC analysis resulted in the almost complete disappearance of this peak (Fig. 6B). If a large excess of GSH was added to the 35% ACN–0.05 M sodium phosphate buffer (pH 7.5) prior to redissolving the dehydrated material, the disappearance of this peak was minimal over the 1-hr period (chromatogram not shown). These results were consistent with the previously observed behavior of synthetic GS-ANIT.

Verification of the peak with a retention time of 11.0 min as GS-ANIT was made by rapid scanning of the HPLC post-column effluent from 250 to 350 nm with a photodiode-array UV detector. This enabled the UV spectrum of this peak to be obtained and compared to that generated by synthetic GS-ANIT. For the sake of comparison, the UV spectrum of the GS-ANIT standard was obtained both during HPLC analysis of synthetic GS-ANIT itself as well as following the addition of an aliquot of synthetic GS-ANIT to a sample of ANIT-treated hepatocytes. In all three instances, the UV absorbance of the material responsible for producing a peak with a retention time of 11.0 min was very similar to that seen previously with GS-ANIT (Fig. 4).

Based on the HPLC peak area, the amount of GS-ANIT in the medium reached a maximum 1.5 hr after the addition of ANIT to the cells (Fig. 6, inset). In comparison to the initial concentration of intracellular GSH, the amount of GS-ANIT in the medium at 2 hr represented <10% of the GSH that was lost from the cells.

The peak identified as GS-ANIT was not observed in samples obtained from untreated hepatocytes or from samples of cell-free medium containing ANIT. Since the majority of peaks visible in samples of ANIT-treated hepatocytes (see Fig. 6) were also observed in samples of cell-free medium containing ANIT, these most likely result from the reaction of ANIT with the various constituents of the incubation medium. As noted in Fig. 6, besides the 11.0 min peak, the peaks with retention times of 8.5, 13.5, and 17.0 min were absent or significantly

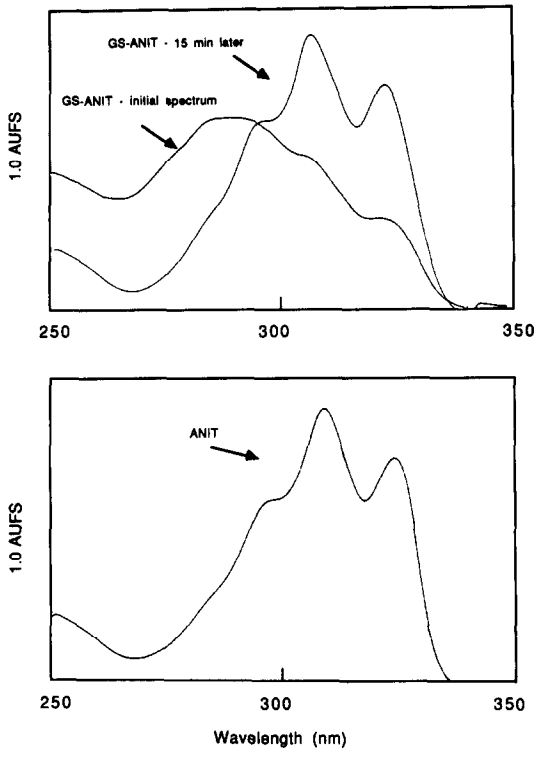

Fig. 4. UV spectra of GS-ANIT and ANIT. The UV spectrum of GS-ANIT both immediately following its dissolution in 20% ACN–0.05 M sodium phosphate (pH 7.5) and 15 min later is depicted (top). For the sake of comparison, the UV spectrum of an equimolar amount of ANIT dissolved in 20% ACN–0.05 M sodium phosphate (pH 7.5) is also shown (bottom). Samples of GS-ANIT which were dissolved in 20% ACN–0.1% acetic acid (pH < 3.5) showed little change over a 15-min period (spectrum not shown).

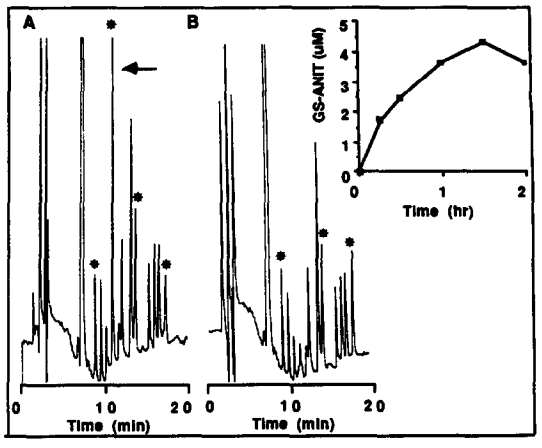

Fig. 6. HPLC analysis of GS-ANIT in incubations of hepatocytes. Hepatocytes (5×10^6/mL) were incubated with ANIT (1 mM) for 2 hr and the presence of GS-ANIT in samples of medium taken at various time points was confirmed by HPLC. (A) Sample was dissolved in 35% ACN, 1.0 M sodium acetate buffer (pH 4.0) prior to injection. (B) Sample was dissolved in 35% ACN, 0.05 M sodium phosphate buffer (pH 7.5) for 1 hr prior to injection. The chromatograms, which were generated by monitoring the post-column effluent at 308 nm, are representative of samples taken at 15 min. The peak designated by the arrow co-chromatographed with that of a GS-ANIT standard. The peaks designated by asterisks were not observed in samples of untreated hepatocytes or cell-free medium containing ANIT. Inset: Time course of appearance of GS-ANIT. Peak area integration was used to calculate the concentration of GS-ANIT in the medium at various time points. N = 3 for each time point. Error bars are obliterated by the symbols.

smaller in samples of untreated hepatocytes and samples of cell-free medium containing ANIT. These peaks may therefore represent other metabolites of ANIT or products of the reaction of ANIT with material exuded by hepatocytes into the medium. In contrast to GS-ANIT, the size of these peaks did not diminish if the sample was dissolved in a buffer at pH 7.5 prior to HPLC analysis.

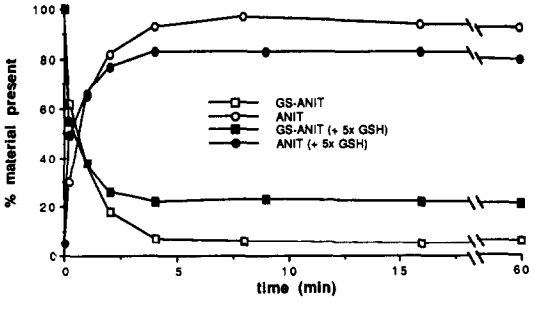

Fig. 5. Kinetics of GS-ANIT disappearance. GS-ANIT (0.15 mM final concentration) was dissolved in either 35% ACN–0.05 M sodium phosphate (pH 7.5) without GSH (open symbols) or with a 5-fold excess of GSH (0.75 mM) (closed symbols). At various times, aliquots were removed and analyzed by HPLC in order to determine the concentration of GS-ANIT and ANIT.

Toxicity of GS-ANIT towards hepatocytes. When exposed to synthetic GS-ANIT, cells exhibited changes similar to those exposed to equimolar amounts of ANIT (compare Fig. 7 with Fig. 1). Incubation with 100 or 500 μM GS-ANIT produced a marked depletion of intracellular GSH over the course of the experiment. Whereas the depletion caused by 100 μM GS-ANIT occurred rapidly and was sustained at approximately 35% of control for several hours, GSH was totally depleted after 3 hr of treatment with 500 μM GS-ANIT. As seen in Fig. 7B, 500 μM GS-ANIT, but not 100 μM GS-ANIT, produced toxicity as assessed by LDH leakage. Although the same dose of ANIT (500 μM) was required to cause toxicity (see Fig. 1), the magnitude of LDH leakage was greater in cells treated with ANIT (90%) than with GS-ANIT (55%).

DISCUSSION

The results of this study indicate that ANIT produced a concentration- and time-dependent depletion of GSH in isolated hepatocytes. The existence of a temporal relationship between LDH leakage and the level of GSH depletion incurred by nontoxic and toxic doses of ANIT suggests that the

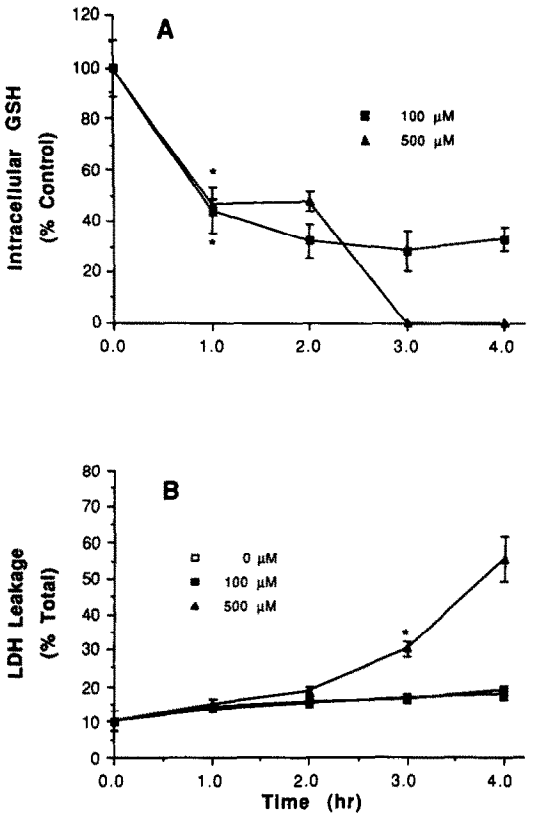

Fig. 7. Effect of GS-ANIT on (A) GSH content and (B) LDH leakage from isolated hepatocytes. Hepatocytes were treated with GS-ANIT (0, 100 or 500 μM) and were analyzed for intracellular GSH and LDH leakage as described in the legend to Fig. 1. The average amount of total LDH released by the cells was 1.995 units/mL. The initial GSH level was 19.2 ± 3.6 nmol/10^6 cells. Data are means ± SEM, N = 3 for each group. Key: (*) significantly different from control at this and subsequent time points ($P < 0.05$).

mechanism by which ANIT caused toxicity is associated with GSH depletion. In cells treated with a nontoxic concentration (100 μM), intracellular GSH decreased to about 25% of the initial value, whereas GSH was totally depleted in cells treated with a toxic concentration (500 μM). Cytotoxicity occurred in hepatocytes only after intracellular GSH fell below 10–15% of the initial value, which is the amount normally associated with mitochondria [27–30].

When hepatocytes are treated with various oxidants, GSH is utilized by the cell as a means of detoxifying hydroperoxides. As a result, GSH is oxidized to GSSG, which, in turn, is exported out of the cell. ANIT did not appear to deplete GSH via this mechanism, for it failed to induce lipid peroxidation or increase GSSG release from the cells. The majority of intracellular GSH which was lost from cells exposed to ANIT was present in the medium as GSH or a GSH-releasing compound. These results suggest that ANIT may deplete cells of GSH by promoting its transport or leakage from the cells or by virtue of its ability to form a reversible conjugate.

Results of our experiments *in vitro* indicate that GS-ANIT was produced when ANIT and GSH were mixed together at room temperature and physiological pH. Results of experiments with this compound revealed that in the absence of GSH (at pH 7.5), the majority (>95%) of GS-ANIT reverted to GSH and ANIT within 5 min. This sharply contrasts with the behavior of the GSH conjugates of benzyl and allyl isothiocyanates which at pH 7.5, achieve an equilibrium where > 85% of the initial compound remains conjugated with GSH [20]. These differences are surprising in view of the structural similarities of ANIT and benzyl isothiocyanate, but may explain why previous investigators were able to detect the mercapturate in urine of animals treated with benzyl isothiocyanate and not with ANIT [19].

Under conditions designed to maximize the formation and stability of GS-ANIT during sample collection and analysis we were able to detect this metabolite in medium of hepatocytes treated with ANIT. Because results of our experiments suggested that the reaction of ANIT with GSH was readily reversible under conditions of our hepatocyte incubation, we hypothesized that administration of an equimolar amount of GS-ANIT to hepatocytes would produce a similar degree of GSH depletion and cell death as that of ANIT. As with ANIT, 500 μM GS-ANIT was required to cause severe GSH depletion and cell death. Although the time scale of appearance of toxicity was similar between the two agents, GS-ANIT caused slightly less LDH leakage from the cells than ANIT. A possible explanation for this result is that GSH released from the conjugate had some cellular protective effect. Since GSH conjugates are unable to enter hepatocytes [31], it is also possible that less ANIT entered cells that were treated with GS-ANIT than cells treated with ANIT. However, because of the extreme propensity of the GSH conjugate to revert to ANIT and GSH, the latter possibility is somewhat unlikely.

Although conjugation of agents with GSH is generally regarded as a means of detoxification, in the past few years it has become increasingly evident that GSH conjugation can sometimes result in bioactivation [32]. Some reactive GSH conjugates such as the *S*-2-(haloethyl)glutathione conjugates do not require further bioactivation to cause toxicity. Metabolism of stable GSH conjugates by γ-glutamyltranspeptidase and other dipeptidases to nephrotoxic cysteine conjugates has also been demonstrated [33, 34]. Mercapturates which are formed by further metabolism of cysteine conjugates are also toxic to the kidney [35]. As GS-ANIT dissociates rapidly to ANIT and GSH, it is unlikely that this conjugate produced toxicity directly or was metabolized to a toxic cysteine conjugate or mercapturate. As suggested by Van Bladeren and associates [20], reversible GSH conjugates such as those formed with benzyl and allyl isothiocyanate may produce toxicity by serving as transport agents for the toxic parent compounds. As they hypothesized, conjugation with GSH might lead to a different

distribution of the parent compound through the body and a propensity towards toxicity occurring at distant sites where GSH concentration is low or where conditions favor the release of the free agent. Because GSH conjugates are secreted avidly into bile [36, 37], conjugation of ANIT with GSH may serve to promote ANIT accumulation in bile. Accumulation of ANIT by this mechanism may explain why biliary epithelial cells are targets for ANIT toxicity *in vivo*. These cells may also be extremely sensitive to the GSH-depleting ability of ANIT, as they contain two-thirds less GSH than hepatocytes [38]. Additional studies designed to address these possibilities are currently in progress.

Although secretion of bile acids into bile is a primary driving factor for the osmotic gradient which drives bile flow, results of numerous studies suggest that GSH contributes to this process. Agents that promote GSH secretion into bile (e.g. furosemide) stimulate bile flow [39, 40], whereas agents that cause GSH oxidation (e.g. *t*-butylhydroperoxide) or depletion (e.g. BSO) lead to a decrease in bile flow [39–42]. Results of our experiments suggest that ANIT depleted hepatocytes of GSH by conjugation. Therefore, the decrease in bile flow which may be afforded by depletion of intracellular GSH by ANIT may be compensated for by an increase in bile flow caused by the added presence of the GSH conjugate in bile. However, it is possible that secretion of the reversible GS-ANIT conjugate into bile may promote cholestasis by increasing ANIT exposure to biliary epithelial cells. This mechanism may explain why both administration of sulfhydryl reagents and a depletion of hepatic GSH reportedly protect animals against ANIT-induced cholestasis [17, 18]. Sulfhydryl reagents could protect hepatocytes and/or biliary epithelial cells from the effects of GSH-depletion caused by ANIT, thereby preserving junctional integrity and bile acid secretion. Conversely, depletion of cellular GSH by BSO may inhibit formation of GS-ANIT and therefore lead to a decrease in the biliary excretion of GS-ANIT. This, in turn, may spare biliary epithelial cells of the toxic effects of ANIT. Clearly, additional experiments need to be performed to adequately address these possibilities.

The demonstration that inducers of cytochrome P450 (i.e. phenobarbital) enhance and that inhibitors (i.e. SKF 525-A, piperonyl butoxide) ameliorate ANIT-induced cholestasis and hyperbilirubinemia suggests that metabolism by cytochrome P450 is required for ANIT to produce liver toxicity [12–14]. These results imply that neither ANIT nor GS-ANIT is directly involved in the mechanism of cholestasis. However, in addition to inducing cytochrome P450, phenobarbital increases GSH *S*-transferase activity and GSH secretion in hepatocytes [39, 43]. Although we did not demonstrate that the conjugation of ANIT with GSH occurred enzymatically as well as nonenzymatically, compounds with similar structure (allyl and benzyl isothiocyanate) undergo enzymatic and nonenzymatic conjugation with GSH [19]. Therefore, we believe enzymatic conjugation of ANIT with GSH is likely to occur within cells. Accordingly, an increase in GSH *S*-transferase activity afforded by phenobarbital could lead to an increase in GS-ANIT formation and a concomitant decrease in GSH in hepatocytes and/or epithelial cells. As seen in Fig. 5, the stability of the conjugate was increased by adding GSH to the incubation medium. An increase in GSH secretion caused by phenobarbital could, therefore, increase the concentration of GS-ANIT in bile. Since the aforementioned cytochrome P450 inhibitors inhibit GSH *S*-transferase activity and/or decrease hepatic GSH content [44–46], it is possible that these agents may protect against ANIT toxicity *in vivo* by inhibiting the formation of GS-ANIT. Therefore, direct involvement of ANIT or GS-ANIT in cholestasis should not be discounted based on results of experiments with cytochrome P450 inducers or inhibitors. Nor do we believe that our results discount involvement of cytochrome P450 metabolism in ANIT toxicity. It is possible that a toxic metabolite of ANIT bound to GSH or some other moiety could be formed during or after metabolism of ANIT by cytochrome P450. The presence of several peaks in the chromatogram of the medium from ANIT-treated hepatocytes suggests that several other metabolites of ANIT may be formed in the liver. Clearly, identification of these metabolites is necessary before the role of metabolism in ANIT toxicity can be fully understood.

In conclusion, results of our experiments suggest that ANIT depletes hepatocytes of GSH *in vitro* by virtue of its ability to form a reversible GSH conjugate. Severe GSH depletion occurs prior to cell death, suggesting that GSH depletion is involved in the pathogenesis of ANIT toxicity to isolated hepatocytes. Whether GSH depletion and/or formation of GS-ANIT is involved in the mechanism of ANIT-induced cholestasis is a matter which remains to be addressed.

Acknowledgements—We thank Marda Brown and Brian Arbogast for technical assistance and Carolyn Knapp for critical reading of the manuscript. This study was supported by NIEHS Grants ES00040 and ES00210. L.C.-D. is the recipient of an individual National Research Service Award (1F32 ESO5483-01).

REFERENCES

1. Lopez M and Mazzanti L, Experimental investigations of alpha-naphthyl-iso-thiocyanate as a hyperplastic agent of the biliary ducts in the rat. *J Pathol Bacteriol* **69**: 243–250, 1955.
2. McLean MR and Rees KR, Hyperplasia of bile-ducts induced by *alpha*-naphthyl-*iso*-thiocyanate: Experimental biliary cirrhosis free from biliary obstruction. *J Pathol Bacteriol* **76**: 175–189, 1958.
3. Goldfarb S, Singer EJ and Popper H, Experimental cholangitis due to alpha-naphthyl-isothiocyanate (ANIT). *Am J Pathol* **40**: 685–698, 1962.
4. Plaa GL and Priestly BG, Intrahepatic cholestasis induced by drugs and chemicals. *Pharmacol Rev* **28**: 207–272, 1977.
5. Kan KS and Coleman R, 1-Naphthylisothiocyanate-induced permeability of hepatic tight junctions of proteins. *Biochem J* **238**: 323–328, 1986.
6. Krell H, Metz J, Jaeschke H, Hoke H and Pfaff E, Drug-induced intrahepatic cholestasis. Characterization of different pathomechanisms. *Arch Toxicol* **60**: 124–130, 1987.

7. Steiner JW and Baglio CM, Electron microscopy of the cytoplasm of parenchymal liver cells in α-naphthylisothiocyanate-induced cirrhosis. *Lab Invest* **12**: 765–790, 1963.
8. Gopinath C and Ford EJH, The effect of alpha-naphthyl isothiocyanate on the liver of sheep and calves. *J Pathol* **100**: 269–280, 1970.
9. Schaffner F, Scharnbeck HH, Hutterer F, Denk H, Greim HA and Popper H, Mechanism of cholestasis. VII. α-Naphthylisothiocyanate-induced jaundice. *Lab Invest* **28**: 321–331, 1973.
10. El-Hawari AM and Plaa GL, Impairment of hepatic mixed-function oxidase activity by α- and β-naphthylisothiocyanate: Relationship to hepatotoxicity. *Toxicol Appl Pharmacol* **48**: 445–458, 1979.
11. Leonard TB, Popp JA, Graichen ME and Dent JG, α-Naphthylisothiocyanate induced alterations in hepatic drug metabolizing enzymes and liver morphology: Implications concerning anticarcinogenesis. *Carcinogenesis* **2**: 473–482, 1981.
12. Roberts RJ and Plaa GL, Potentiation and inhibition of α-naphthylisothiocyanate-induced hyperbilirubinemia and cholestasis. *J Pharmacol Exp Ther* **150**: 499–506, 1965.
13. Roberts RJ and Plaa GL, Effect of norethandrolone, acetohexamide, and envoid on α-naphthylisothiocyanate-induced hyperbilirubinemia and cholestasis. *Biochem Pharmacol* **15**: 333–341, 1966.
14. Horky J, Grasso P and Golberg L, Influence of phenobarbital on histological and biochemical changes in experimental intrahepatic cholestasis. *Exp Pathol* **5**: 200–211, 1971.
15. Roberts RJ, Pharm B and Plaa GL, The effect of bile duct ligation, bile duct cannulation, and hypothermia on α-naphthylisothiocyanate-induced hyperbilirubinemia and cholestasis in rats. *Gastroenterology* **50**: 768–774, 1966.
16. Cappizo F and Roberts RJ, α-Naphthylisothiocyanate (ANIT)-induced hepatotoxicity and disposition in various species. *Toxicol Appl Pharmacol* **19**: 176–187, 1971.
17. El-Hawari AM and Plaa GL, α-Naphthylisothiocyanate (ANIT) hepatotoxicity and irreversible binding to rat liver microsomes. *Biochem Pharmacol* **26**: 1857–1866, 1977.
18. Dahm LJ and Roth RA, Protection against α-naphthylisothiocyanate-induced liver injury by decreased hepatic non-protein sulfhydryl content. *Biochem Pharmacol* **42**: 1181–1188, 1991.
19. Brusewitz G, Cameron BD, Chasseaud LF, Gorler K, Hawkins DR, Koch H and Mennicke WH, The metabolism of benzylisothiocyanate and it cysteine conjugate. *Biochem J* **162**: 99–107, 1977.
20. Bruggeman IM, Temmink JHM and van Bladeren PJ, Glutathione- and cysteine-mediated cytotoxicity of allyl and benzyl isothiocyanate. *Toxicol Appl Pharmacol* **83**: 349–359, 1986.
21. Fariss MW, Brown MK, Schmitz JA and Reed DJ, Mechanism of chemical-induced toxicity. I. Use of a rapid centrifugation technique for the separation of viable and nonviable hepatocytes. *Toxicol Appl Pharmacol* **79**: 283–295, 1985.
22. Reed DJ, Babson JR, Beatty PW, Brodie AE, Ellis WW and Potter DW, High performance liquid chromatography analysis of nanomole levels of glutathione, glutathione disulfide, and related thiols and disulfides. *Anal Biochem* **106**: 55–62, 1980.
23. Erwin BG, Stoscheck CM and Florini JR, A rapid fluorimetric method for the estimation of DNA in cultured cells. *Anal Biochem* **110**: 291–294, 1981.
24. Amador E, Dorfman LL and Walker WEC, Serum lactate dehydrogenase (LDH) activity–Analytical assessment of current assays. *Clin Chem* **9**: 391–399, 1963.
25. Stacey NH and Klaassen CD, Copper toxicity in isolated rat hepatocytes. *Toxicol Appl Pharmacol* **58**: 211–220, 1981.
26. Fariss MW and Reed DJ, Measurement of glutathione and glutathione disulfide efflux from isolated rat hepatocytes. In: *Isolation, Characterization, and Use of Hepatocytes* (Eds. Harris, RA and Cornell NW), pp. 349–355. Elsevier, Amsterdam, 1983.
27. Meredith MJ and Reed DJ, Status of the mitochondrial pool of glutathione in the isolated hepatocyte. *J Biol Chem* **257**: 3747–3753, 1982.
28. Olafsdottir K, Pascoe GA and Reed DJ, Mitochondrial glutathione status during Ca^{2+} ionophore-induced injury to isolated hepatocytes. *Arch Biochem Biophys* **263**: 226–235, 1988.
29. Jocelyn P, Some properties of mitochondrial glutathione. *Biochim Biophys Acta* **396**: 427–436, 1975.
30. Younes M and Siegers C-P, Mechanistic aspects of enhanced lipid peroxidation following glutathione depletion *in vivo*. *Chem Biol Interact* **34**: 257–266, 1981.
31. Sies H, Wahlländer A, Waydhas C, Soboll S and Haberle D, Functions of intercellular glutathione in hepatic hydroperoxide and drug metabolism and the role of extracellular glutathione. *Adv Enzyme Regul* **18**: 303–320, 1980.
32. Igwe OJ, Biologically active intermediates generated by the reduced glutathione pathway: Toxicological implications. *Biochem Pharmacol* **35**: 2987–2994, 1986.
33. Elfarra AA and Anders MW, Renal processing of glutathione conjugates: Role in nephrotoxicity. *Biochem Pharmacol* **33**: 3729–3732, 1984.
34. Monks TJ and Lau SS, Commentary: Renal transport processes and glutathione conjugate-mediated nephrotoxicity. *Drug Metab Dispos* **15**: 437–441, 1987.
35. Commandeur JNM, Brakenhoff JPG, de Kanter FJJ and Vermeulen NPE, Nephrotoxicity of mercapturic acids of three structurally related 2,2-difluoroethylenes in the rat. *Biochem Pharmacol* **37**: 4495–4504, 1988.
36. Barnhart JL and Combes B, Choleresis associated with metabolism and biliary excretion of diethyl maleate in the rat and dog. *J Pharmacol Exp Ther* **206**: 614–623, 1978.
37. Wahlländer A and Sies H, Glutathione *S*-conjugate formation from 1-chloro-2,4-dinitrobenzene and biliary *S*-conjugate excretion in the perfused rat liver. *Eur J Biochem* **96**: 441–446, 1979.
38. Parola M, Cheeseman KH, Biocca ME, Dianzani MU and Slater TF, Menadione and cumene hydroperoxide induced cytotoxicity in biliary epithelial cells isolated from rat liver. *Biochem Pharmacol* **39**: 1727–1734, 1990.
39. Ballatori N and Truong AT, Relation between biliary glutathione excretion and bile acid-independent bile flow. *Am J Physiol* **256**: G22–G30, 1989.
40. Akerboom TPM, Bilzer M and Sies H, Relation between glutathione redox changes and biliary excretion of taurocholate in perfused rat liver. *J Biol Chem* **259**: 5838–5843, 1984.
41. Akerboom TPM, Bultmann T and Sies H, Inhibition of biliary taurocholate excretion during menadione metabolism in perfused rat liver. *Arch Biochem Biophys* **263**: 10–18, 1988.
42. Ballatori N and Truong AT, Altered hepatic junctional permeability, bile acid secretion and glutathione efflux during oxidant challenge. *J Pharmacol Exp Ther* **251**: 1069–1075, 1989.
43. Kaplowitz N, Eberle DE, Petrini J, Touloukian J, Corvasce MC and Kuhlenkamp J, Factors influencing the efflux of hepatic glutathione into bile in rats. *J Pharmacol Exp Ther* **224**: 141–147, 1983.

44. Fromowitz P, Brondeau MT, Bonnet P and De Ceaurriz J, Effect of SKF 525-A on the glutathione-conjugating enzyme system and on liver toxicity. *Toxicol Lett* **36**: 275–280, 1987.
45. Hoshi K, Senda N, Igarashi T, Satoh T, Ueno K and Kitagawa H, Effects of co-administration of monomethylaminoantipyrine with diethylaminoethyl-2,2-diphenylvalerate (SKF 525-A) on gamma-glutamyl-transpeptidase, glutathione *S*-transferase, and hepatic drug metabolizing enzyme activities in rats. *Res Commun Chem Pathol Pharmacol* **52**: 71–80, 1986.
46. James RC and Harbison RD, Hepatic glutathione and hepatotoxicity. Effects of cytochrome P-450 complexing compounds SKF 525-A, L-α-acetylmethadol (LAAM), norLAAM, and piperonyl butoxide. *Biochem Pharmacol* **31**: 1829–1835, 1982.